

Theory-based Scaling of Energy Confinement Time for Future Reactor Design

J.M. Park¹, G. Staebler², P.B. Snyder², C.C. Petty², D.L. Green¹, K.J. Law¹

¹Oak Ridge National Laboratory, Oak Ridge, TN, United States

²General Atomics, San Diego, CA, United States

The scaling of thermal energy confinement time plays important roles in tokamak fusion research. A simple log-linear scaling from regression analysis of a large experimental database has been widely used in terms of the engineering or dimensionless parameters. A particularly important example is the IPB98(y,2) scaling for ELMMy H-mode plasmas developed for the ITER project [1].

$$\tau_{98(y,2)} = 0.056 I_p^{0.93} B_T^{0.15} n_e^{0.41} P^{-0.69} R^{1.97} \epsilon^{0.58} \kappa_a^{0.78}.$$

Here, $\tau_{98(y,2)}$ = thermal energy confinement time [sec], I_p = plasma current [MA], B_T = toroidal magnetic field [T], n_e = line average density [$10^{19}/m^3$], P = loss power [MW], R = major radius [m], ϵ = a/R , a = minor radius [m], $\kappa_a = V/2\pi^2 a^2 R$, V = plasma volume [m^3]. This experimental scaling derived from a multi-machine database is a fundamental tool for transport studies of present day experiments and forms a basis for the design of future reactors such as FNSF and DEMO beyond ITER. The system design code usually employs this experimental scaling (or its variants) with an assumption of the confinement enhancement factor, H ($=\tau/\tau_{98(y,2)}$) to optimize the reactor design parameters. One of the primary limitations of this approach is that the optimum design parameters depend strongly on the desired value of H . Moreover, the experimental scaling from the present-day experiments might not be valid in burning plasma conditions with electron dominant heating, low rotation, and low collisionality, which might result even in a wrong optimization path for the reactor design.

In this work, a theory-based scaling of thermal energy confinement time has been derived based on a comprehensive turbulent transport model TGLF [2] in core coupled to the EPED [3] edge pedestal model, especially in burning plasma conditions with dominant fusion alpha particle heating for future reactor design. The simulation dataset consists of a massive number of predictive IPS-FASTRAN [4] simulations, self-consistent with core transport, edge pedestal, fusion alpha particle heating, and MHD equilibrium, built upon a modern integrated modeling framework, Integrated Plasma Simulator (IPS). The IPS-FASTRAN modeling finds a steady-state ($d/dt=0$) solution of electron density (n_e), electron temperature (T_e), ion

temperature (T_i), and toroidal rotation (Ω) with turbulent radial fluxes predicted by TGLF with the SAT0 saturation rule in addition to neoclassical transport from the Chang-Hinton model. Boundary conditions are applied at the pedestal top, where $\rho = 1-3/2w_{ped} = \rho_{ped}^{top}$ with the values predicted by IPS-EPED1, where ρ is the normalized minor radius proportional to the square root of the toroidal flux and w_{ped} is the full width of the edge pedestal. The electron density profile for $\rho_{ped}^{top} < \rho < 1$ is taken from the EPED1 model profile with a hyperbolic tangent shape in the pedestal. The value at the separatrix of $\rho=1$ is assumed $n_e^{sep} = 1/2n_e^{ped}$, where both n_e^{ped} and n_e^{sep} are input of EPED1. The temperatures for $\rho_{ped}^{top} < \rho < 1$ are updated by assuming, $n_e T_e = n_i T_i = 1/2 P_{EPED1}$, where P_{EPED1} is the total pressure predicted by EPED1. Note that the ion density n_i is calculated by the charge balance with the calculated value of Z_{eff} . The Helium ash density profile is calculated by $n_{He}(\rho)/5\tau_E = S_a(\rho)$, where τ_E is the calculated thermal energy confinement time, S_a is fusion alpha particle production rate. ITER-like impurity models for Ar and Be are applied: $n_{Ar} = 0.0005 \times n_e$, $n_{Be} = 0.02 \times n_e$.

The DAKOTA-enabled IPS framework generates the multi-dimensional parametric scan with random sampling of major radius ($4 < R < 8$ m), aspect ratio ($2.5 < R/a < 3.5$), elongation ($1.5 < \kappa < 2.0$), triangularity ($0.3 < \delta < 0.6$), toroidal magnetic field ($4 < B_T < 8$ T), plasma current ($3.5 < q_{95} < 8.5$), line average density ($0.6 < n_e / n_{GW} < 1$), and heating power ($20 < P_{inj} < 150$ MW). The following analytic form of the double null plasma shape is used: $R_b(\theta) = R + a \cos(\theta + \sin^{-1}(\delta \sin \theta))$, $Z_b(\theta) = \kappa a \sin(\theta)$. Each IPS-FASTRAN simulation in the scan is largely theory-based except a model specification of the heating and plasma current profiles. A Gaussian form of the heating profile is employed with the ratio of electron and ion heating as an additional scan parameter ($0.0 < P_e/P_i < 1.0$) to take into account difference in the heating and current drive actuators such as neutral beam injection and RF heating. The model current profile is a combination of the bootstrap current in the edge pedestal determined by EPED and the core current profile parameterized to make variation of minimum q (q_{min}), the minimum q location (ρ_{qmin}), and the average magnetic shear ($q_0 - q_{min}$) in the core, where the Sauter models is employed for the bootstrap current calculation.

For the ITER baseline H-mode type current profile with $q_0 \sim 1.0$ (black line of Fig 1(a)), the TGLF/EPED energy confinement time scales as

$$\tau_{TGLF/EPED} = 0.098 I_p^{0.80} B_T^{0.28} n_e^{0.42} P^{-0.71} R^{2.1} \kappa^{0.81} \epsilon^{0.90},$$

in a dimensionally homogenous form [5], showing $\sim +/- 10\%$ difference in average from the IPB98(y,2) scaling $\tau_{98(y,2)}$ for the data set generated in burning plasma condition as shown in Fig 2. It should be noted that the exponent of the log-linear scaling expression reveals

different dependency on the engineering variables, for example stronger (weaker) dependency on B_T (I_p). Figure 3 shows comparison between $\tau_{TGLF/EPED}$ and $\tau_{98(y,2)}$ from one dimensional scan around the ITER values, where the other engineering parameters are fixed at $R = 6$ m, $a = 2$ m, $B = 5$ T, $\kappa = 1.85$, $\delta = 0.5$, $n_e/n_{GW} = 1$, $P = 100$ MW.

The $\tau_{TGLF/EPED}$ scaling can be transformed with dimensionless parameters as

$$\Omega_i \tau_{TGLF/EPED} \sim \rho^{* -2.63} \beta^{-1} v_C^{0.04} q^{-2.75} \epsilon^{1.08} \kappa^{3/2},$$

showing the normalized gyroradius ρ^* scaling between Bohm and gyro-Bohm ($\rho^{-2.63}$), weak collisionality dependency ($v_C^{0.04}$), and unfavorable beta dependency (β^{-1}), generally consistent with the IPB(y,2) scaling. Here, Ω_i is cyclotron frequency and q is safety factor.

Substantial improvement of thermal energy confinement time is predicted for the broader current profile. Figure 1 also shows the calculated profiles of the electron and ion temperatures between the monotonic q profile with $q_0 \sim 1$ (black) and broader current profile (red) with a weak magnetic shear at $\rho(q_{min}) \sim 0.6$ (red), otherwise at the same conditions for the $R = 4$ m and $B_T = 7$ T reactor, showing that the confinement time is a strong function of the q profiles. The broader current profile leads to the confinement enhancement $H = \tau_{TGLF/EPED}/\tau_{98(y,2)} > 1$ as shown in Fig 2 (red symbols). A larger dataset with variation of the current profiles suggests $\tau_{TGLF/EPED} \sim (1 + 0.45\rho_{qmin}^{1.2})$, identifying an optimization path to AT steady-state reactor.

The accuracy of the log-linear fit shown in Fig 4 can be improved with an advanced regression method such as a neural network, which will be eventually coupled to the system code such as GASC and PROCESS.

- [1] McDonald et al, Nucl. Fusion **47**, 147 (2007)
- [2] Staebler, et al, Phys. Plasmas **14**, 055909 (2007)
- [3] Snyder et al, Nucl. Fusion **51**, 103016 (2011)
- [4] Park et al, Phys. Plasmas **25**, 012506 (2018)
- [5] Luce et al, Plasma Phys. Control. Fusion **50** 043001(2008)

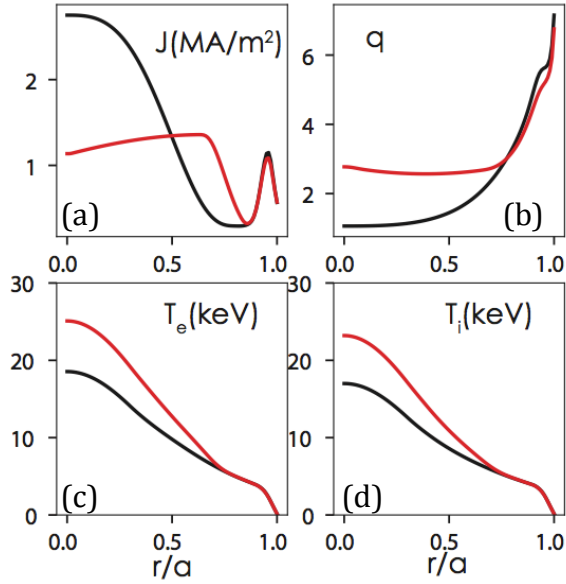


Fig 1. Confinement dependency on the current profile (black: monotonic q profile with $q(0) \sim 1$, red: broad current profile with $q_{\min} > 2$)

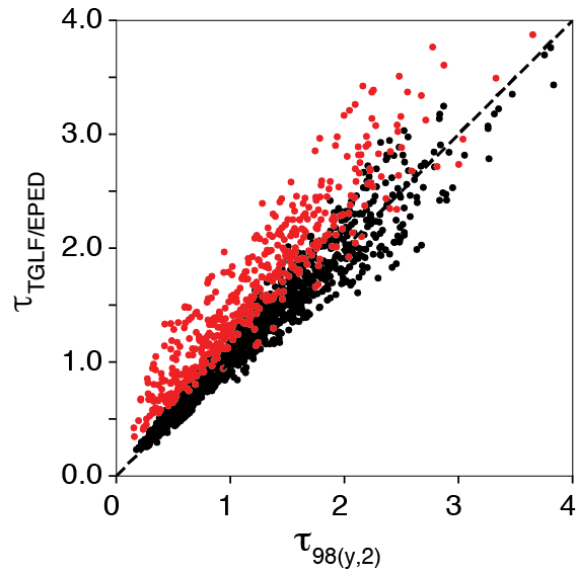


Fig 2. Theory-based energy confinement time vs experimental scaling (black: monotonic, red: broad current profile)

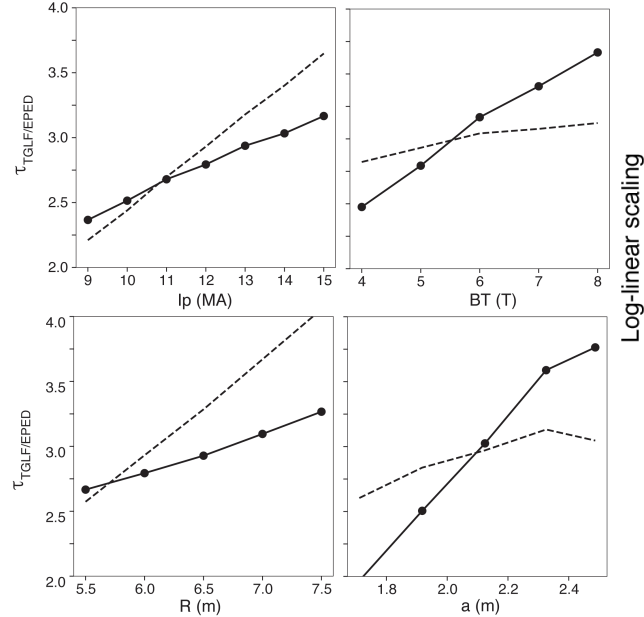


Fig 3. Difference between the theory-based and experimental scaling of energy confinement time (solid: theory-based, dash: experimental)

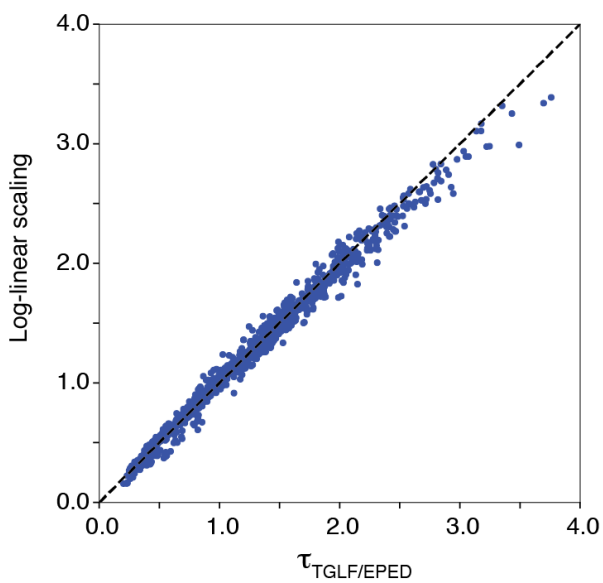


Fig 4. Accuracy of the log-linear scaling of $\tau_{\text{TGLF/EPED}}$